Available online at www.sciencedirect.com
ScienceDirect
Journal of Nuclear Materials 367–370 (2007) 848–852
journal of nuclear materials
www.elsevier.com/locate/jnucmat

Effect of 2 wt% Ti addition on high-temperature strength of fine-grained, particle dispersed V–Y alloys

H. Kurishita [a,*], S. Oda [b], S. Kobayashi [b], K. Nakai [b], T. Kuwabara [c], M. Hasegawa [a], H. Matsui [a]

[a] *International Research Center for Nuclear Materials Science, Institute for Materials Research (IMR), Tohoku University, Oarai, Ibaraki 311-1313, Japan*
[b] *Department of Materials Science and Engineering, Ehime University, Matsuyama 790-8577, Japan*
[c] *Electronics and Materials R&D Laboratories, Sumitomo Electric Industries Ltd., Osaka Works, 1-1-3, Shimaya, Konohana-ku, Osaka 554-0024, Japan*

Abstract

In order to examine the effects of 2 wt% Ti addition on microstructures and room- and high-temperature strengths for fine-grained, particle dispersed V–Y alloys, a V–1.7Y–2.1Ti (in wt%) alloy was fabricated by powder metallurgical (P/M) methods. Microstructural examinations were made by transmission electron microscopy (TEM). Tensile tests were performed at temperatures from room-temperature to 1273 K at initial strain rates from 1×10^{-5} to 1×10^{-2} s^{-1}. The results were compared with those of V–(1.7–2.4)Y and V–4Cr–4Ti (NIFS heat-1) alloys. TEM examinations showed that 2.1% Ti addition provides an extended capability of maintaining a fine-grained structure in P/M V–Y alloys with larger interparticle distance. Tensile test results indicated that the high-temperature yield strength of V–1.7Y–2.1T is considerably higher than expected from the grain-size dependence of the yield strength, and that the deformation controlling mechanism is essentially the same as that for V–1.7Ti. The observed effects of Ti addition are discussed.

1. Introduction

Improvements in both the resistance to embrittlement by neutron irradiation and the strength at high-temperatures are key issues for use of V and its alloys as fusion structural materials [1–5]. Recent progress on microstructural control by advanced powder metallurgical (P/M) methods made it possible to fabricate ultra-fine-grained, particle dispersed V–Y alloys with good ductility by removing solute impurities of oxygen and nitrogen from the matrix [6–8]. It has been reported that the features of these V–Y alloys are a stable microstructure up to 1573 K, solute (oxygen and nitrogen) free matrix phase, good ductility in the as-HIPed state (no plastic working), good resistance to neutron irradiation to 0.25 and 0.60 dpa at 563 K and 873 K, and a strong temperature dependence of yield strength [7–11].

As a result of the strong temperature dependence of yield strength up to around 1023 K, V–(1.7–2.4)Y (in wt%) alloys exhibited higher strengths than

* Corresponding author. Tel.: +81 29 267 4157; fax: +81 29 267 4947.
E-mail address: kurishi@imr.tohoku.ac.jp (H. Kurishita).

0022-3115/$ - see front matter © 2007 Elsevier B.V. All rights reserved.
doi:10.1016/j.jnucmat.2007.03.071

V–4Cr–4Ti (NIFS heat-1). The microstructures introduced in V–(1.7–2.4)Y alloys are hence expected to be effective in improving the high-temperature strength of V–4Cr–4Ti. However, above 1173 K V–(1.7–2.4)Y alloys showed lower strengths than the solution hardened V–4Cr–4Ti alloy. Deformation mechanism studies showed that the deformation mode of V–Y alloys has changed from a recovery controlled process of the long-range internal stress field to grain boundary sliding [11]. In view of the significance of the contribution of solution-hardening to high-temperature strengths, it is reasonable to suggest that the lower strength of the alloys is mainly attributable to the occurrence of grain boundary sliding, based on very fine grains and much less solution-hardening.

Titanium is known to be an effective solution-hardening element in vanadium. It is hence worth examining effects of Ti addition on the microstructures and mechanical properties of fine-grained, particle dispersed V–Y alloys, however no such studies have been reported. In this work, a V–1.7Y–2.1Ti (wt%) alloy with fine grains and finely dispersed particles was fabricated by P/M methods and evaluated by TEM/EDX microstructural examinations and tensile tests up to 1273 K.

2. Experimental

Powders of unalloyed V (particle size: <150 μm, O: 0.08 wt%, N: 0.07 wt%), Y (<750 μm, 1.56 wt%, 0.05 wt%) and Ti (78 μm, 0.29 wt%, 0.01 wt%) were used as the starting materials. They were mixed to provide the nominal composition of V–1.7Y–2.1Ti (in wt%) in a glove box filled with a purified Ar gas (purity 99.99999%). The mixed powder was charged into two vessels made of WC/Co and then subjected to mechanical alloying (MA). MA treatments were conducted by a planetary ball mill for 50 h in a purified Ar (purity 99.99999%) atmosphere. The details of MA processes are reported elsewhere [8]. HIP was conducted at 1273 K and 200 MPa for 3 h in an Ar atmosphere. From the as-HIPed compacts, specimens for microstructural observations by transmission electron microscopy (TEM), X-ray diffraction (XRD) analyses and tensile tests were prepared. The dimensions of the tensile specimens were $16\,\text{mm} \times 4\,\text{mm} \times 0.5\,\text{mm}$ with the gauge section of $5\,\text{mm} \times 1.2\,\text{mm} \times 0.5\,\text{mm}$, with the shoulder section designed to support the applied load [8]. All of the specimens were wrapped with Ta foil and then Zr foil and annealed at 1273 K for 1 h in a vacuum better than 5×10^{-5} Pa. Table 1 shows the designation and chemical composition of the specimens. The contents of W and Mo arising from the milling vessels and balls during MA are also shown.

Tensile tests were performed at room-temperature and temperatures from 873 to 1273 K at initial strain rates of 1×10^{-5} to $1 \times 10^{-2}\,\text{s}^{-1}$. High-temperature tensile tests were conducted in a vacuum better than 3×10^{-4} Pa with Ta and Zr foils used for additional protection of the specimens from pick-up of gaseous impurities during the test. Details of the tests were reported elsewhere [11].

Fracture surfaces of the tensile-tested specimens were examined by scanning electron microscopy (SEM) with a JSM-5400. Microstructural examinations and EDX analyses were by transmission electron microscopy (TEM) using a JEM-2000FX operating at 200 kV. XRD analyses to identify the dispersed compound particles used a voltage of 30 kV and current of 250 mA.

3. Results and discussion

3.1. Microstructure

XRD analyses showed that the peaks of Y and Ti were clearly observed in the mixed powder, whereas they completely disappeared in the MA processed powder and the value of 2θ corresponding to the peak of V(1 1 0) shifted to a lower angle. This peak shift stems from lattice expansion caused by supersaturation with Y [8] and Ti, indicating that Y and Ti dissolved into the V matrix during MA. After HIP and the subsequent annealing peaks of Y_2O_3 and YN were clearly observed, which were

Table 1
Designation and chemical compositions of developed V–1.7Y–2.1Ti and V–Y alloys [11] (wt%)

Specimen	Y	Ti	O	N	C	H	Mo	Co	W
V–1.7Y–2.1Ti	1.74	2.05	0.160	0.084	0.019	0.0002	–	–	0.015
V–1.7Y	1.68	–	0.187	0.104	0.127	0.0001	–	0.026	0.272
V–1.9Y	1.92	–	0.321	0.073	0.029	0.0001	0.15	–	–
V–2.4Y	2.37	–	0.566	0.083	0.027	0.0001	3.35	–	–

due to the reaction of solute impurities of O and N with dissolved Y during HIP [6–8]. No appreciable differences were observed in the XRD patterns for V–1.7Y–2.1Ti and V–1.7Y [8], except for a slight decrease in peak heights for V–1.7Y–2.1Ti due probably to the smaller contents of O and N in Table 1.

TEM bright and dark field images and EDX analyses revealed grain structures and the size distribution of dispersed particles. The average diameters of grains and dispersed particles and the number density of dispersed particles for V–1.7Y–2.1Ti are listed in Table 2, where the results for V–1.7Y, V–1.9Y and V–2.4Y [11] are also included. Comparison of the result of V–1.7Y–2.1Ti with that of V–1.7Y shows that the 2.1% Ti addition increases the average grain-size and decreases the particle number density. This indicates that the grain-size of the alloys is determined by the pinning effect of the dispersed particles. In addition, TEM/EDX analysis at grain interiors where no particles were observed showed that approximately 1 wt% Ti is in solution. The remaining Ti content of approximately 1 wt% was found to contribute to oxide formation.

Fig. 1 shows the relationship between the average grain-size and the center-to-center inter-particle spacing for V–1.7Y–2.1Ti and V–Y alloys. It should be noted that 2.1% Ti addition provides an extended capability of maintaining a fine-grained structure of the P/M V–Y alloys with larger inter-particle distance.

3.2. Tensile properties

Fig. 2 shows stress–strain curves at room-temperature at an initial strain rate of 1×10^{-3} s^{-1} for each vanadium alloy. Comparison of the result of V–1.7Y–2.1Ti with that of V–1.7Y shows that 2.1% Ti addition decreases the yield and tensile strengths from 580 to 490 MPa and from 630 to 550 MPa, respectively, but increases the uniform and total elongation from 7% to 10% and from 15% to 20%, respectively. The yield and tensile strengths of V–1.7Y–2.1Ti are still approximately 1.5 times higher than those of V–4Cr–4Ti.

Table 2
Microstructural parameters for V–1.7Y–2.1Ti and V–Y alloys [11]

Designation	Mean grain diameter (nm)	Particle (10^{20}/m^3)	Mean particle diameter (nm)
V–1.7Y–2.1Ti	518	6.0	14.7
V–1.7Y	339	31.3	12.9
V–1.9Y	504	12.6	16.8
V–2.4Y	268	71.6	13.5

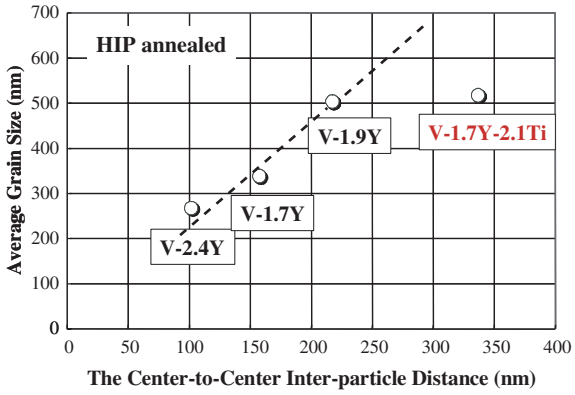

Fig. 1. Relationship between the average grain-size and the center-to-center inter-particle spacing for V–1.7Y–2.1Ti and V–Y alloys.

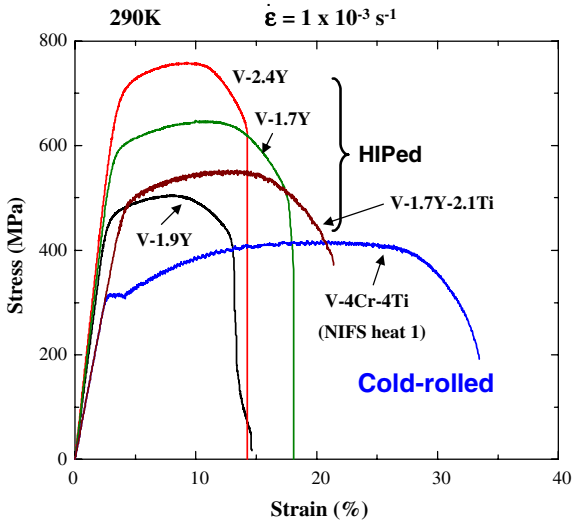

Fig. 2. Stress–strain curves at room-temperature at the initial strain rate of 1×10^{-3} s^{-1} for each V alloy.

Fig. 3 shows a plot of the yield strength against grain-size for the V–1.7Y–2.1Ti and V–Y alloys. Here, the yield strength is normalized to that for V–1.9Y, which is the lowest among the alloys. For the V–Y alloys without Ti addition, the grain-size dependence of the normalized yield strength can be divided into two types depending on temperature; the low-temperature type from RT to 1073 K where the strength increases with decreasing grain-size (grain-size strengthening), and the high-temper-

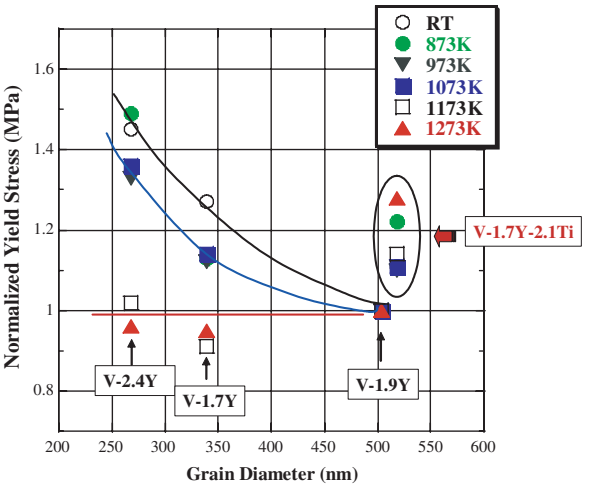

Fig. 3. Normalized yield strength as a function of grain-size for V–1.7Y–2.1Ti and V–Y alloys deformed at various temperatures at 1×10^{-3} s^{-1}.

ature type above 1173 K where the strength does not change with decreasing grain-size. It should be noted from Fig. 3 that the normalized yield strength for V–1.7Y–2.1Ti is considerably higher than that expected from the above grain-size dependence for the V–Y alloys, especially at 1273 K. Since V–1.7Y–2.1Ti had the lowest number density of dispersed particles and thus the smallest contribution of dispersion hardening to the flow stress, it is reasonable to state that the observed increase in the normalized yield strength for V–1.7Y–2.1Ti is attributable to solution-hardening by Ti. In view of the significant enhancement of the normalized yield strength at 1273 K, Ti in solution may have a beneficial effect of suppressing grain boundary sliding, as discussed later.

In order to identify the deformation controlling mechanism, the test temperature and strain rate dependence of the yield strength was examined. The results are shown in Fig. 4, together with the data on the V–Y alloys. An Arrhenius plot of the yield strength shows that V–1.7Y–2.1Ti exhibits behavior similar to V–1.7Y; i.e., at temperatures from around 923 to near 1173 K, the data points for both the alloys lie on lines with similar slope, whereas the data points at 1273 K deviate from the lines and appear to fall on a curve close to the straight line connecting the data points at 1173 and 1273 K for V–2.4Y. Therefore, the effect of plastic strain rate on yield strength was examined at 1073 K for V–1.7Y–2.1Ti, V–1.7Y and V–2.4Y and at 1273 K for V–2.4Y.

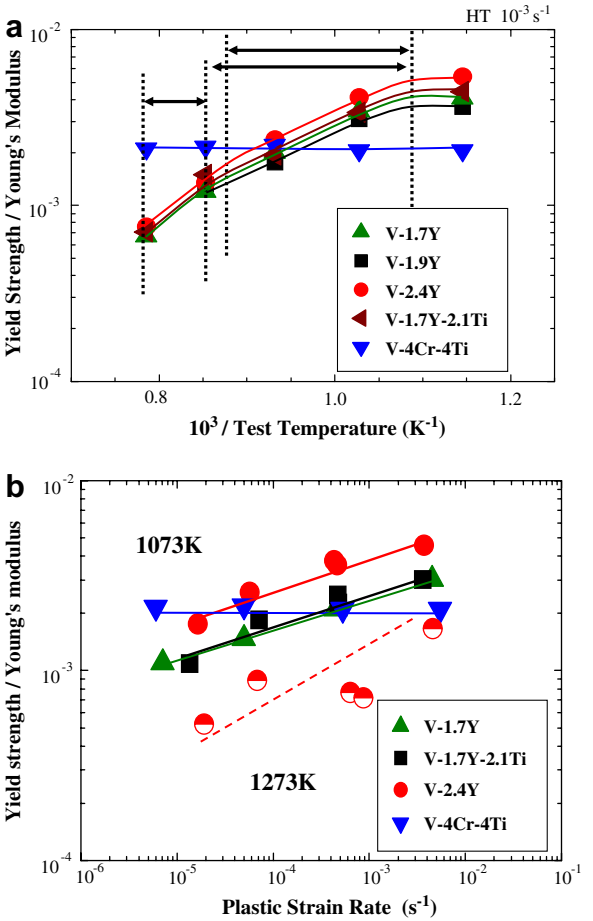

Fig. 4. (a) Arrhenius plot of yield strength at 1×10^{-3} s^{-1} and (b) plastic strain rate dependence of yield strength at 1073 and 1273 K for each V alloy.

Table 3 lists the stress exponent of strain rate, n, and the activation energy for deformation, Q_d. The values of approximately 6.0 and 280 kJ/mol for V–1.7Y–2.1Ti are slightly smaller than those for V–1.7Y, but they are still close to the case of high-temperature deformation of bcc pure metals, where the n value is approximately 5 and the Q_d value corresponds to the activation energy for self-diffusion

Table 3
Stress exponent of plastic strain rate, n, and the activation energy for deformation, Q_d, for V–1.7Y–2.1 Ti and for V–Y alloys

	Temperature range (K)	Stress exponent, n	Activation energy, Q_d (KJ/mol)
V–1.7Y–2.1Ti	973–1173	5.7	281
V–1.7Y	973–1173	6.4	306
V–2.4Y	973–1153	5.4	263
V–2.4Y	>1153	2.8	183

in pure V, 308 kJ/mol [12]. Therefore, we can say that the deformation between 973 and 1173 K for V–1.7Y–2.1Ti is controlled by recovery of obstacles with long-range internal stress fields. On the other hand, the mechanism controlling the deformation above 1173 K for V–1.7Y–2.1Ti is not yet identified, however, the observed significant decrease in yield strength at 1273 K may be related to grain boundary sliding. The results above 1153 K for V–2.4Y in Table 3 are distinctly smaller than those for the above recovery control and may suggest that the deformation is controlled by a grain boundary associated mechanism, such as grain boundary sliding. V–2.4Y had the smallest grain-size and is hence prone to grain boundary sliding.

Grain boundary sliding may require the movement of associated dislocations. It is well known that in solution hardened alloys solute atmospheres are formed around dislocations at high-temperatures. For the dislocations with solute atmosphere to move at high-temperatures the dislocations must experience solute atmosphere dragging, which is called the solute atmosphere dragging mechanism. Solute atmosphere dragging may suppress the movement of dislocations and therefore grain boundary sliding. This is believed to be the reason why the normalized yield strength for V–1.7Y–2.1Ti increased at high-temperatures, especially at 1273 K. This, in turn, indicates that for further improvement in high-temperature strength, the development of fine-grained V alloys with more solution-hardening may be effective.

4. Conclusions

A V–1.7Y–2.1Ti alloy with fine grains and finely dispersed particles of Y_2O_3 and YN was prepared by P/M methods, including MA-HIP processing, followed by annealing at 1273 K. Microstructural examinations by TEM/EDX and XRD and tensile tests at room- and high-temperatures from 873 to 1273 K at initial strain rates from 1×10^{-5} to $1\times10^{-2}\,s^{-1}$ were performed. The results were compared to results for V–(1.7–2.4)Y alloys without Ti additions and to V–4Cr–4Ti (NIFS heat-1). The main results are as follows:

(1) 2.1% Ti addition provides an extended capability for maintaining a fine-grained structure in P/M V–Y alloys with larger inter-particle distance.
(2) 2.1% Ti addition decreases the yield and tensile strengths, but increases the uniform and total elongation at room-temperature.
(3) The high-temperature yield stress of V–1.7Y–2.1T is considerably higher than expected from the grain-size dependence of the yield stress of V–Y alloys without Ti addition, especially at 1273 K. This strength increase of V–1.7Y–2.1T is attributed to solution-hardening by Ti.
(4) The high-temperature deformation mechanism for V–1.7Y–2.1Ti is essentially the same as that for V–1.7Y.
(5) Increase in solution-hardening effects is expected to contribute to improvement in high-temperature strength of ultra-fine-grained V alloys.

Acknowledgements

The authors would like to express their gratitude to Professors T. Muroga and T. Nagasaka at NIFS for their supply of V–4Cr–4Ti (NIFS heat-1), to Dr H. Arakawa, IMR, Tohoku University, for his help with use of HIP apparatus and to Dr S. Matsuo for his review of the paper.

References

[1] S.J. Zinkle, H. Matsui, D.L. Smith, A.F. Rowcliffe, E. van Osch, K. Abe, V.A. Kazakov, J. Nucl. Mater. 258–263 (1998) 205.
[2] L.L. Snead, S.J. Zinkle, D.J. Alexander, A.F. Rowcliffe, J.P. Robertson, W.S. Eatherly, Fusion Materials Semiannual Progress Report DOE/ER-0313/23, 1997, p. 81.
[3] T. Muroga, T. Nagasaka, A. Iiyoshi, A. Kawabata, S. Sakurai, M. Sakata, J. Nucl. Mater. 283–287 (2000) 711.
[4] T. Nagasaka, T. Muroga, M. Imamura, S. Tomiyama, M. Sakata, Fusion Technol. 39 (2001) 659.
[5] T. Muroga, T. Nagasaka, K. Abe, V.M. Chernov, H. Matsui, D.L. Smith, Z.-Y. Xu, S.J. Zincle, J. Nucl. Mater. 307–311 (2002) 547.
[6] T. Kuwabara, H. Kurishita, M. Hasegawa, J. Nucl. Mater. 283–287 (2000) 611.
[7] H. Kurishita, T. Kuwabara, M. Hasegawa, S. Kobayashi, K. Nakai, J. Nucl. Mater. 343 (2005) 318.
[8] T. Kuwabara, H. Kurishita, M. Hasegawa, Mater. Sci. Eng. A 417 (2006) 16.
[9] S. Kobayashi, Y. Tsuruoka, K. Nakai, H. Kurishita, Mater. Trans. 45 (2004) 9.
[10] S. Kobayashi, Y. Tsuruoka, K. Nakai, H. Kurishita, J. Nucl. Mater. 329–333 (2005) 447.
[11] S. Oda, H. Kurishita, Y. Tsuruoka, S. Kobayashi, K. Nakai, H. Matsui, J. Nucl. Mater. 329–333 (2004) 462.
[12] Metal Data Book, 3rd Ed., The Japan Institute of Metals, 1993, p. 24.